

Computerized Method for Evaluating the Suitability of Trailing Cables

JOHN M. MESINA

Abstract- In response to a problem encountered in the field, the Approval and Certification Center initiated a program to develop models which enable computer calculation of conductor temperature rise versus time in trailing cables. To date, a common model equation has been developed and parameters determined for two round trailing cables typically used on continuous miners, Type G-GC, sizes 2/0 AWG and 4/0 AWG, rated 90°C. The resulting cable models have been tentatively confirmed in laboratory trials using repetitive four-level constant current cycles and triangular currents in which the peak current varied on succeeding cycles. Model refinement and additional laboratory trials are projected using randomly varying current, simulating actual current conditions in mine trailing cables. Contingent on success here, trials on an operating continuous miner will follow.

I. Introduction

WHEN A CABLE conducts fluctuating current which occasionally exceeds the cable's ampacity rating, overheating will recur if adequate cooling is not afforded by the timing. In most mining applications, trailing cable currents are best described as cyclic random in which the instantaneous current often exceeds the cable's ampacity. This is especially true for continuous miners in which motor current is influenced by nebulous variables such as conditions of the face, bit sharpness, and the individual operator's control technique. Such situations engender uncertainty when specifying a trailing cable. The uncertainty is reduced somewhat by recognizing that the life of a mine trailing cable rarely exceeds one year, due primarily to physical damage, whereas the life expectancy of a protected stationary cable operated at rated current is 20 to 30 years; accordingly, some overheating seems tolerable. However, when the temperature-elevating variables act in concert, unacceptable severe overheating can occur.

On one occasion an investigation revealed that the average conductor temperature of a continuous miner's trailing cable, rated at 90°C, exceeded 120°C during the last quarter of the place-cutting interval. This miner was operated by remote control on an unusually rocky face, and considerable motor jamming occurred during sump and downcut. The cable jacket was very hot to the touch (73 °C maximum), indicating the need for corrective measures.

Paper IC 88-30, approved by the Mining Industry Committee of the IEEE Industry Applications Society for presentation at the Ninth West Virginia University International Mining Electrotechnology Conference, Morgantown, WV, July 26-29, 1988. Manuscript released for publication March 1, 1989. The author is with the electrical Power Systems Branch, approval and Certification Center, Mine Safety and Health Administration, U.S. Department of the Interior, Industrial Park Road, RR1, Box 251, Triadelphia, WV 26059

One possible correction is to increase the trailing cable size, but calculating the size adequate to lower the temperature is problematic. A reliable algorithm is needed. The algorithm must be based on a mathematical model relating conductor (conductor insulation) temperature to any time-varying current. A literature search failed to uncover the desired model, and therefore, this program was initiated.

II. TECHNICAL APPROACH

A graph of current (i) versus time (t) in a continuous miner trailing cable [1] lends little encouragement when attempting to define the multitudinous current variations thereon by a single equation. Repeatable patterns are not to be found. The graph is actually a series connection of current waveforms - none of which duplicates the waveform preceding or following it. However, each waveform can be defined mathematically. For example: $i = I$ (constant) for motor stall or idling, and $i = i_0 + at$ at $i_0 =$ current at time zero, $a =$ slope) for a ramp waveform. In general, any order polynomial of t is conceivable.

The complexity of random current duty led to the following reasoning: if an equation could be developed which predicts the rise of conductor temperature (T_c) above ambient temperature (T_a), i.e., ($T_c - T_a$), versus time for any of the possible series current waveforms, the temperature rise calculated at the end time of one waveform would serve as the initial temperature condition for the following waveform calculation. Starting with a known conductor temperature, successive application of the equation would theoretically monitor the conductor temperature rise thereafter. Such tedious calculations require a computer. Since the algorithm requires presetting the computer with the individual current waveform equation before starting each calculation of the series, real-time calculation would not be possible. However, "if the various currents could be described by a common means, the computer would be able to simply receive signals from a current sensor (and an ambient temperature sensor, if the ambient varies) and, in real time, calculate conductor temperature.

A. Cable Model

A lumped-parameter cable model patterned after that of Melsom and Booth [2] and Cox [3] was chosen to represent round cables. The model combines the heat dissipating effects of conduction, convection, and radiation into a single thermal transfer term. The model also lumps the heat absorbing

parameters, i.e., the masses and specific heat capacities of the cable components. With these simplifications the cable appears to be a single copper conductor which instantaneously converts current into heat energy which is conducted away through a single insulating mass, the innermost temperature of which is T_c and the outer temperature of which is T_a . For a unit length of cable:

c	specific heat capacity ($W \cdot \text{min}/\text{kg} \cdot ^\circ\text{C}$),
i	instantaneous 60 Hz rms value of current (A_{rms}),
i (subnotation)	denotes initial value,
i	initial value of i (A_{rms}),
$i(t)$	i expressed in terms of time (A_{rms}),
i_r	i at time T (A_{rms}),
I	constant current,
I_m	rms value of $i(t)$ for the "calculation interval" (A_{rms}),
K_c	conductor's (resistance/temperature) ratio ($\Omega/^\circ\text{C}$),
K_0	thermal transfer coefficient ($W/^\circ\text{C}$), (note: K_c and K_0 values are assumed constant for a given cable),
$2m$	insulating mass (kg) (note: $2m$ is used in lieu of the customary m to facilitate typing),
Q	heat energy ($W \cdot \text{min}$),
R	instantaneous conductor resistance (Ω),
t	time (min), ($t = 0$ to $t = T$) "calculation interval" (min),
T_a	ambient air temperature ($^\circ\text{C}$),
T_{avg}	average temperature of the insulating mass ($^\circ\text{C}$),
T_c	conductor temperature at time t ($^\circ\text{C}$),
T_i	initial ($t = 0$) conductor temperature ($^\circ\text{C}$).

The instantaneous input and output heat rates are

$$\frac{dQ_{\text{in}}}{dt} = i^2 R \quad (1)$$

and

$$\frac{dQ_{\text{out}}}{dt} = K_0(T_c - T_a). \quad (2)$$

At equilibrium (steady state) the input and output heat rates are equal. When the conductor temperature is in transition, an absorption heat rate term (dQ_{abs}/dt) adjusts the average temperature of the cable mass. Assuming a temperature gradient such that the average mass temperature (T_{avg}) is

$$T_{\text{avg}} = \frac{T_c + T_a}{2} = \frac{T_c - T_a}{2} + T_a,$$

the time rate of energy absorbed (or given up) by the mass is

$$\begin{aligned} \frac{dQ_{\text{abs}}}{dt} &= (2m)c \frac{dT_{\text{avg}}}{dt} \\ &= mc \left[\frac{d(T_c - T_a)}{dt} + 2 \frac{dT_a}{dt} \right]. \end{aligned}$$

Unlike the model of [2] and [3], T_a is treated as a variable with respect to time. T_a can change with time due to normal workplace variation and with T_c if T_a is measured too close to the cable jacket. To assume T_a is constant simplifies the mathematics, but this precludes the effect of variable T_a on both the absorption and output heat rates. If instead T_a is measured sufficiently far from the cable to ensure that $2 dt_a$ is insignificant relative to $d(T_c - T_a)$,

$$\frac{dQ_{\text{abs}}}{dt} = mc \frac{d(T_c - T_a)}{dt}. \quad (3)$$

Since

$$\frac{dQ_{\text{abs}}}{dt} = \frac{dQ_{\text{in}}}{dt} - \frac{dQ_{\text{out}}}{dt}, \quad (4)$$

$$mc \frac{d(T_c - T_a)}{dt} = i^2 R - K_0(T_c - T_a). \quad (5)$$

Through use of the inferred-zero resistance concept [4], R may be written as

$$R = K_c[(T_c - T_a) + (T_a + 234.5)]. \quad (6)$$

Combining (5) and (6) yields

$$\begin{aligned} \frac{d(T_c - T_a)}{dt} &= (i^2) \frac{K_c}{mc} [(T_c - T_a) + (T_a + 234.5)] \\ &\quad - \frac{K_0}{mc} (T_c - T_a). \quad (7) \end{aligned}$$

An attempt was made to solve $T_c - T_a$ for general $i(t)$ from (7) in the following manner: defining

$$U = \frac{d(T_c - T_a)}{dt}, \quad (8)$$

$$\begin{aligned} \frac{du}{d(T_c - T_a)} &= \frac{K_c}{mc} i^2 \left[1 + \frac{dT_a}{d(T_c - T_a)} \right] \\ &\quad + [(T_c - T_a) + (T_a + 234.5)] \frac{di(t)^2}{d(T_c - T_a)} - \frac{K_0}{mc}. \quad (9) \end{aligned}$$

Since $2dT_a \ll d(T_c - T_a)$ has been assumed,

$$\begin{aligned} \frac{du}{d(T_c - T_a)} &= \frac{K_c}{mc} i^2 + [(T_c - T_a) + T_a + 234.5] \\ &\quad \cdot \frac{di(t)^2}{d(T_c - T_a)} - \frac{K_0}{mc}. \quad (10) \end{aligned}$$

Proceeding in this manner does not result in a general solution of $T_c - T_a$ but only in the identity

$$\begin{aligned} T_c - T_a &= \left[(T_i - T_{ai}) \frac{A_i}{A} - \frac{T_{ai} + 234.5}{\frac{K_0}{K_c} - i_T^2} \right] i_0^2 e^{x e^z} \\ &\quad + \frac{T_a + 234.5}{\frac{K_0}{K_c} - i_T^2} i_T^2. \quad (11) \end{aligned}$$

in which $T_c - T_a$ is the conductor temperature rise during the calculation interval (0 to T) and

$$\frac{A_i}{A} = \frac{1 - \frac{K_c}{K_0} i_0^2}{1 - \frac{K_c}{K_0} i_T^2} \quad (12)$$

$$x = \frac{-K_0}{mc} \int_0^T \left[1 - \frac{K_c}{K_0} i(t)^2 \right] dt \quad (13)$$

$$z = \frac{K_c}{mc} \int_0^T (T_c - T_a + T_a + 234.5) \left[\frac{di(t)^2/dt}{d(T_c - T_a)/dt} \right] dt. \quad (14)$$

Equation (14) presents calculation difficulty in that z becomes discontinuous whenever $T_c - T_a$ is constant. Also, since $T_c - T_a$ appears in the equation, calculation must involve iteration. The complexity lent by (14) compels attention to alternate methods.

The literature [5] provides an alternate approach to solving (7) when T_a is held constant

$$T_c - T_a = e^{-\int_0^t P(t) dt} \left[C_1 - \int_0^t q(t) e^{P(t) dt} dt \right]$$

in which

$$P(t) = \frac{K_0}{mc} \left[1 - \frac{K_c}{K_0} i(t)^2 \right] \quad (16)$$

$$q(t) = \frac{-K_c}{mc} (T_a + 234.5) i(t)^2 \quad (17)$$

and

C_1 = integration constant, condition: $T = \text{constant}$.

Equation set (15)-(17) seems to preclude real-time solution for random multiple series current waveforms; it appears the computer would have to predict and preset itself on each new waveform.

Enlightened of the complexity of (11)-(14) and the (assumed) limitation of (15)-(17), attention was turned toward simplification. Equation (14) resists simplification, but for constant current, $z = 0$, and (11)-(14) becomes (18), (19):

$$T_c - T_a = \left[T_i - T_a - \frac{T_a + 234.5}{\frac{K_0}{K_c} - I^2} I^2 \right] e^x + \frac{T_a + 234.5}{\frac{K_0}{K_c} - I^2} I^2 \quad (18)$$

where

$$x = -\frac{K_0}{mc} \left[1 - \frac{K_c}{K_0} I^2 \right] T, \quad \text{condition: } i = \text{constant}. \quad (19)$$

(Note that (18), (19) also results when (15)-(17) is solved for the case $i(t) = I$.) Since any current waveform may be approximated by a sequence of short-duration constant currents, (18), (19) may be used to calculate $T_c - T_a$ in real time.

An alternate simplification means is to substitute I_{rms} for i in (1). Defining

$$I_{\text{rms}} = \left[\frac{\int_0^T i(t)^2 dt}{T} \right]^{1/2} = \text{average effective current during the calculation interval}, \quad (20)$$

the substitution thus incorporates an averaging mechanism in the input heat rate, and (7) and (10) become (21) and (22), respectively:

$$\frac{d(T_c - T_a)}{dt} = I_{\text{rms}}^2 \frac{K_c}{mc} [(T_c - T_a) + (T_a + 234.5)] - \frac{K_0}{mc} (T_c - T_a) \quad (21)$$

and

$$\frac{du}{d(T_c - T_a)} = \frac{K_c}{mc} I_{\text{rms}}^2 - \frac{K_0}{mc}. \quad (22)$$

Equations (11)-(14) then convert to

$$T_c - T_a = \left[T_i - T_{ai} - \frac{T_a + 234.5}{\frac{K_0}{K_c} - I_{\text{rms}}^2} I_{\text{rms}}^2 \right] e^x + \frac{T_a + 234.54}{\frac{K_0}{K_c} - I_{\text{rms}}^2} I_{\text{rms}}^2 \quad (23)$$

where

$$x = -\frac{K_0}{mc} \left[1 - \frac{K_c}{K_0} I_{\text{rms}}^2 \right] T \quad (24)$$

under the condition that $i = I_{\text{rms}}$, assumed constant in the calculation interval. (Note that (18), (19) result from (23), (24) when the conductor current is constant since then $I_{\text{rms}} = I$.)

For both constant current and ramp current, (20) yields for the calculation interval the relationship

$$I_{\text{rms}}^2 = \frac{i_0^2 + i_0 i_T + i_T^2}{3}. \quad (25)$$

Equation (25) may also be used to 'approximate I_{rms}^2 ' for a waveform of any continuous curvature. This equates to assuming the current follows the chord connecting current values at $t = 0$ and $t = T$, the calculation interval end points. Based on the considerations presented, (23)-(25), were tentatively accepted as the cable model equation, subject to confirmation from dynamic performance trials.

B. Determining Parameters of the Cable Model Equation

Before dynamic trials could be undertaken to test (23)-(25), the values of parameters K_c , K_o , and mc had to be determined. Realizing the difficulty in valuating mc , the concept of a cooling constant was utilized to delete mc as follows. If in (23)-(25), I_{rms} is set equal to zero and T to t (23) becomes the model's pure-cooling equation

$$T_c - T_a = (T_i - T_a)e^{-K_o/mc t}. \quad (26)$$

Defining the cooling time constant t_c as that value of t for which

$$T_c - T_a = (T_i - T_a)e^{-1}, \quad (27)$$

it follows that

$$mc = K_o t_c. \quad (28)$$

t_c is measured by stabilizing the conductor temperature at some level T_i , setting $i = 0$ at $t = 0$, measuring and collecting data ($T_c - T_a$ versus time) as the cable cools, and then locating in the data compilation the time (t_c) at which $T_c - T_a = (T_i - T_a)e^{-1}$.

Equation (28) converts (24) to

$$x = \frac{-\dot{T}}{t_c} \left[1 - \frac{K_c}{K_o} I_{rms}^2 \right]. \quad (29)$$

Substituting (29) for (24) results in the model (23), (25), (29), and only K_o/K_c remains to be measured. Analysis revealed that K_o/K_c could be measured by a variety of methods. Effort was directed to those methods requiring only static (steady-state) measurements as described next.

Equations (23) and (24) reveal that when the current is constant and $T_c - T_a$ no longer varies with time, T_c assumes the value T_f , "f" for final [6], where

$$T_f - T_a = \frac{T_a + 234.5}{\frac{K_o}{K_c} - I^2} I^2. \quad (30)$$

Equation (30) can be rearranged as

$$I^2 = \frac{K_o}{K_c} \left(\frac{T_f - T_a}{T_f + 234.5} \right). \quad (31)$$

Thus linear regression analysis of I^2 versus $(T_f - T_a)/(T_f + 234.5)$ data should ideally result in the line of regression

$$I^2 = A_1 + B_1 \frac{T_f - T_a}{T_f + 234.5} \quad (32)$$

in which $A_1 = 0$ and $B_1 = \text{constant}$, so that

$$\frac{K_o}{K_c} = B_1 \text{ ("Method 1")}, \quad \text{condition: } A_1 = 0. \quad (33)$$

Equation (30) may also be arranged as

$$\frac{1}{T_f - T_a} = \frac{-1}{T_a + 234.5} + \frac{\frac{K_o}{K_c}}{T_a + 234.5} \left(\frac{1}{I^2} \right). \quad (34)$$

If T_a is held constant and K_o/K_c is constant as assumed, (34) represents a line plotting $1/(T_f - T_a)$ versus $1/I^2$ data with intercept at $-1/(T_a + 234.5)$ and with slope equal to $(K_o/K_c)/(T_a + 234.5)$. Linear regression analysis of the data converts the line to the form involving constants A_2 and B_2 :

$$\frac{1}{T_f - T_a} = A_2 + B_2 \left(\frac{1}{I^2} \right). \quad (35)$$

Comparing (34) and (35) indicates two possible definitions for K_o/K_c :

$$\frac{K_o}{K_c} = -\frac{B_2}{A_2} \text{ ("Method 2")}, \quad (36)$$

$$\text{condition: } A_2 = -\frac{1}{T_a + 234.5},$$

and

$$\frac{K_o}{K_c} = B_2(T_a + 234.5) \text{ ("Method 3")}. \quad (37)$$

C. Test Equipment and Conditions

The required test measurements are time, ambient temperature, conductor temperature, and conductor current. Since dynamic as well as static testing was needed, an automatic data collection system was mandatory. To enable comparison of data with similar studies elsewhere, the cable was to be tested in still air at a constant ambient temperature; a sufficiently large test room was chosen to ensure minimal ambient temperature variation while relying essentially on natural convection to dissipate the cable and equipment heat. Two test cables were obtained from Cablec Corporation,¹ 20 feet long, round, 2/0 and 4/0, type G-GC (three conductor), 2000 V, P-102-114 MSHA, ethylene propylene insulation with hypalon jacket. The test cable was laid upon 3 3/4" high wood supports which rested on the floor and were spaced approximately 6 ft apart along the cable length. The cable sat in 3/4" -deep smooth-edged grooves, one in each wood support; accordingly, the distance from the floor to cable bottom was nominally 3 in (closer between supports when the cable sagged due to heat expansion). The floor was ceramic tiled. Type K (chrome alumel) thermocouples, No. 26 AWG, were constructed-insulating up to the bead with heat shrinkable tubing. A thermocouple was imbedded just inside the cable's stranded power conductor. It entered the cable through the apex of a 2- to 3-in-long V-shaped slit in the jacket. One layer of vinyl electrician's tape was wrapped around the slit to secure the thermocouple while approximating a normal cable jacket at the slit. Having been alerted to an "end effect" error from placing the thermocouple too close to the cable termination [1], the thermocouple was located approximately six feet from the power supply terminal. The ambient temperature thermocouple was positioned 4 in to the side of the cable jacket adjacent the conductor thermocouple and level with cable center.

¹ Reference to specific products does not imply endorsement by the Mine Safety and Health Administration.

TABLE I
STATIC TEST DATA, 2/0 AND 4/0 CABLES

2/0, G-GC, Round, 90°			4/0, G-GC, Round, 90°		
T_f (°C)	T_a (°C)	I (A _{rms})	T_f (°C)	T_a (°C)	I (A _{rms})
130.0	25.0	353.6	132.5	25.4	459.6
114.2	24.7	325.3	120.2	25.1	437.8
100.4	25.0	297.6	110.3	25.1	417.7
83.6	24.8	268.8	101.0	24.8	390.6
69.3	23.4	245.0	87.0	24.0	364.9
56.9	22.7	211.4	76.7	23.6	336.9
49.4	23.0	186.4	62.2	23.4	289.5
37.7	22.1	145.5	51.0	22.9	249.5
37.0	22.4	133.6	35.8	22.2	135.9
28.7	22.3	80.1			
24.1	22.2	42.4			

TABLE II
INTERCEPT, SLOPE, AND K_0/K_c VALUES: METHODS 1, 2, AND 3

Cable: 2/0, G-GC, Round, 90°C							
Method	Line Equation	n	Intercept (A_n)	Slope (B_n)	Correlation Coefficient	K_0/K_c Equation	K_0/K_c (W/Ω)
1	31,32	1	-3438	$4.25(10^3)$	0.9979	33	$4.25(10\$)$
2	34,35	2	$-2.044(10^{-3})$	1398	0.9998	36	$6.84(10\$)$
3	34,35	2	$-2.044(10^{-3})$	1398	0.9998	37	$3.59(105)$
Cable: 4/0, G-GC, Round, 90°C							
1	31,32	1	-1291	$7.02(10^3)$	0.9964	33	$7.02(10^3)$
2	34,35	2	$-1.662(10^{-3})$	2316	0.9998	36	$1.394(10^4)$
3	34,35	2	$-1.662(10^{-3})$	2316	0.9998	37	$5.95(105)$

One terminal of a single-phase alternating current power supply (Multi-Amp, Model LBM-75A) was connected to one end of the cable. The cable's three conductors were properly spliced to ensure the same current through each. A 500-A 100-mV calibrated shunt was connected between the cable's opposite end and the power supply. The shunt voltage was fed to a (true rms voltage reading) Hewlett Packard Model 3478A Digital Multimeter. The thermocouples were connected to a Hewlett Packard Model 3497A Data Acquisition Unit, which in turn, along with the output of the rms meter, connected to a Digital Equipment PDP 11/23 Computer by way of a IBV11, IEEE 488 Instrument Interface. An eighth-order polynomial [7], [8] was programmed on the computer to compensate for each thermocouple's inherent non-linearity. The instantaneous current and thermocouple voltages were scanned and recorded every four seconds.

D. Static Testing to Determine K_0/K_c

Tests to determine K_0/K_c consisted of jockeying the current to rapidly stabilize T_a at approximately $T_f = 130^\circ\text{C}$. Thereafter, current was successively reduced and jockeyed rapidly to obtain successively lower T_f values. Table I lists the T_f , T_a , and I values measured for the 2/0 and 4/0 cables. As shown, T_a remained fairly constant (approximately $\pm 1.5^\circ\text{C}$ variation).

Analysis of Table I data revealed that best linearity is obtained for (35) by deleting data points for $T_f = 37.0$, 28.7, and 24.1 (2/0 cable) and for $T_f = 35.8$ (4/0 cable). Since the conductor temperature of operating continuous miners generally exceeds 40°C , the deletions were allowed for calculating K_0/K_c by Methods 2 and 3, which are based on (35).

Table II lists the intercept, slope, and K_0/K_c values determined from (31) through (37) and Table I data. The table shows that discrepancies exist between the K_0/K_c values of Methods 1, 2, and 3 for each cable. Table II also reveals that neither the condition for Method 1 ($A_1 = 0$), nor the condition for Method 2 ($A_2 = -1/(T_a + 234.5) = -3.9 \cdot 10^{-3}$) was obtained. This finding seems to indicate that K_0/K_c is not constant as was assumed for the model. This impression is further supported by solving (34) and (35) simultaneously for K_0/K_c . The result,

$$\frac{K_0}{K_c} = (T_a + 234.5)(B_2 + A_2 I^2) + I^2,$$

appears to indicate that unless $A_2 = -1/(T_a + 234.5)$, K_0/K_c should be treated as variable with I^2 .

E. Dynamic Tests

Tests were conducted next to determine which of the alternate K_0/K_c values worked best in the dynamic mode.

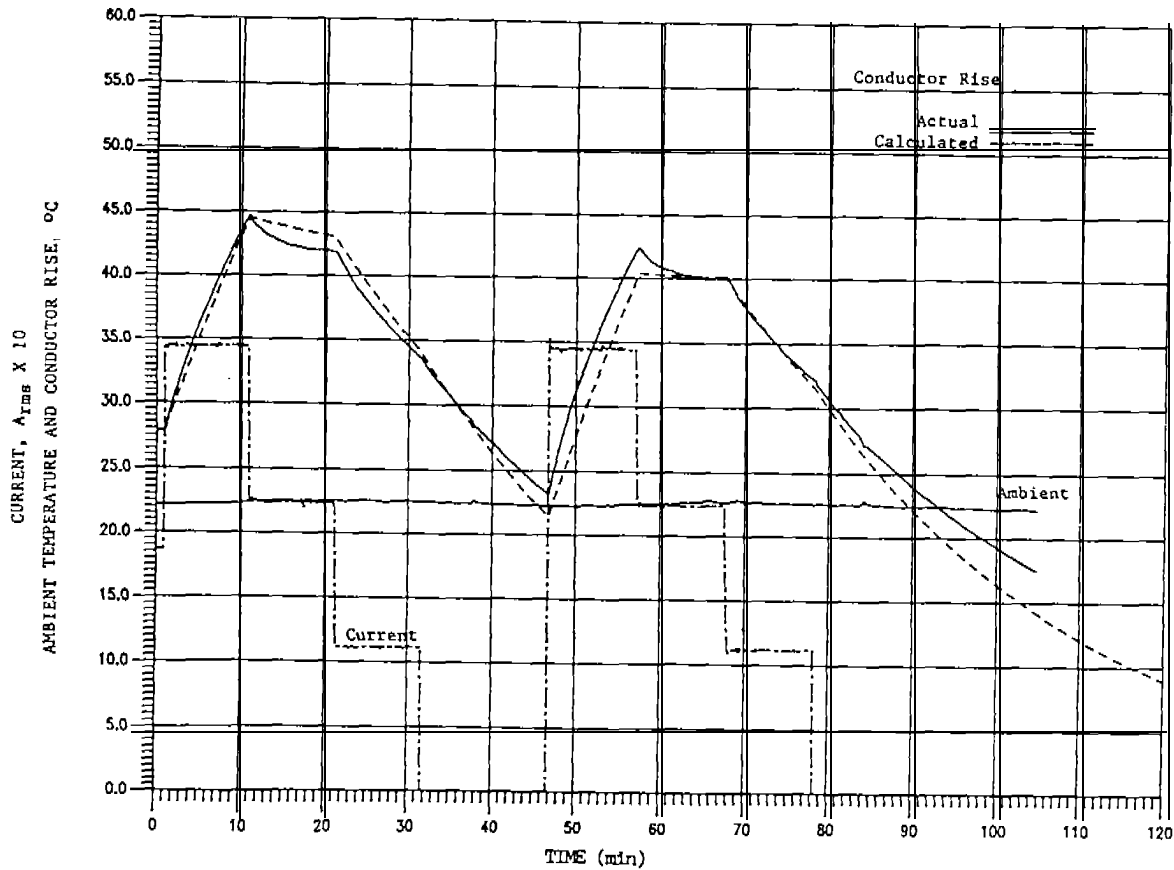


Fig. 1. Conductor temperature rise-four-step "low" current, 2/0 cable, round, type G-GC, 90°C.

Cooling constants were measured first by the method described adjacent (28). By allowing the cables to cool from approximately 130°C, the measured t_c values are 33.1 and 39.1 rein, respectively for the 2/0 and 4/0 cables. Tests were then performed using two cycles of four-level constant-current steps as illustrated on Figs. 14. The actual and the best-fit calculated conductor temperature rises along with ambient temperature are also plotted on the figures. Trial calculations indicated that K_1/K_2 from Method 2 provides the best fit for Figs. 14. Accordingly, the best-fit model equation (combining (23), (29), (30), and (35) and equating I_{rms} to I) is

$$T_c - T_a = \left[T_i - T_{ai} - \frac{I_{rms}^2}{B_2 + A_2 I_{rms}^2} \right] e^{-(T/t_c)[1 + (A_2/B_2)I_{rms}^2]} + \frac{I_{rms}^2}{B_2 + A_2 I_{rms}^2}; \quad (38)$$

$$2/0 \text{ cable: } A_2 = -2.044 (10^{-3})$$

$$B_2 = 1398$$

$$t_c = 33.1 \text{ min;}$$

$$4/0 \text{ cable: } A_2 = -1.662 (10^{-3})$$

$$B_2 = 2316$$

$$t_c = 39.1 \text{ min.}$$

For each dynamic test reported here, T_{ai} and T_a in (38) were

set constant at the lowest T_a value during the test. Equation (25) is used to calculate I_{rms}^2 (note that for a constant current $i_0 = i_T$).

The current step values in Fig. 14 are 0 (bottom level), and 1/3, 2/3, and 1 times I_{max} , where I_{max} values (A_{rms}) are 345 and 524 in Figs. 1 and 2, respectively, for the 2/0 cable, and 460 and 643 in Figs. 3 and 4, respectively, for the 4/0 cable. The current levels just prior to the first steps are the values which stabilized the conductor temperature at 50 °C, approximately 184 A_{rms} for the 2/0 cable and 248 A_{rms} for the 4/0 cable. $T_c - T_{ai}$ was calculated for each succeeding 0.1-rein interval; each calculation interval was 0 to 0.1 min. The new $T_i - T_{ai}$ value was set equal to the calculated $T_c - T_a$ value of the previous calculation. Although the current waveforms are not perfect steps, perfection was assumed for the calculations.

Ramp currents were also used to test (38). The general ramp equation is $i(t) = i_0 + at$. The results of these tests are presented in Figs. 5-8. The conductor temperature is plotted in lieu of conductor temperature rise as in Figs. 1-4; $T_c - T_a$ was calculated from (38), then the lowest measured T_a was subtracted. A calculation was performed for each 0.1-min section. For the ramps employed such a short calculation interval (0.1 rein) is tantamount to assuming $i_0 = i_i$ in (25). By assuming $i_0 = i_i$ in (25) the ramp current waveforms were converted to stepped ramps with 0.1-min duration constant current steps of amplitude i_T . For each succeeding 0.1-min section, ($T_i - T_{ai}$) was set to ($T_c - T_a$) calculated for the previous 0.1-min section, T was set to 0.1 min, and i_0 and i_T

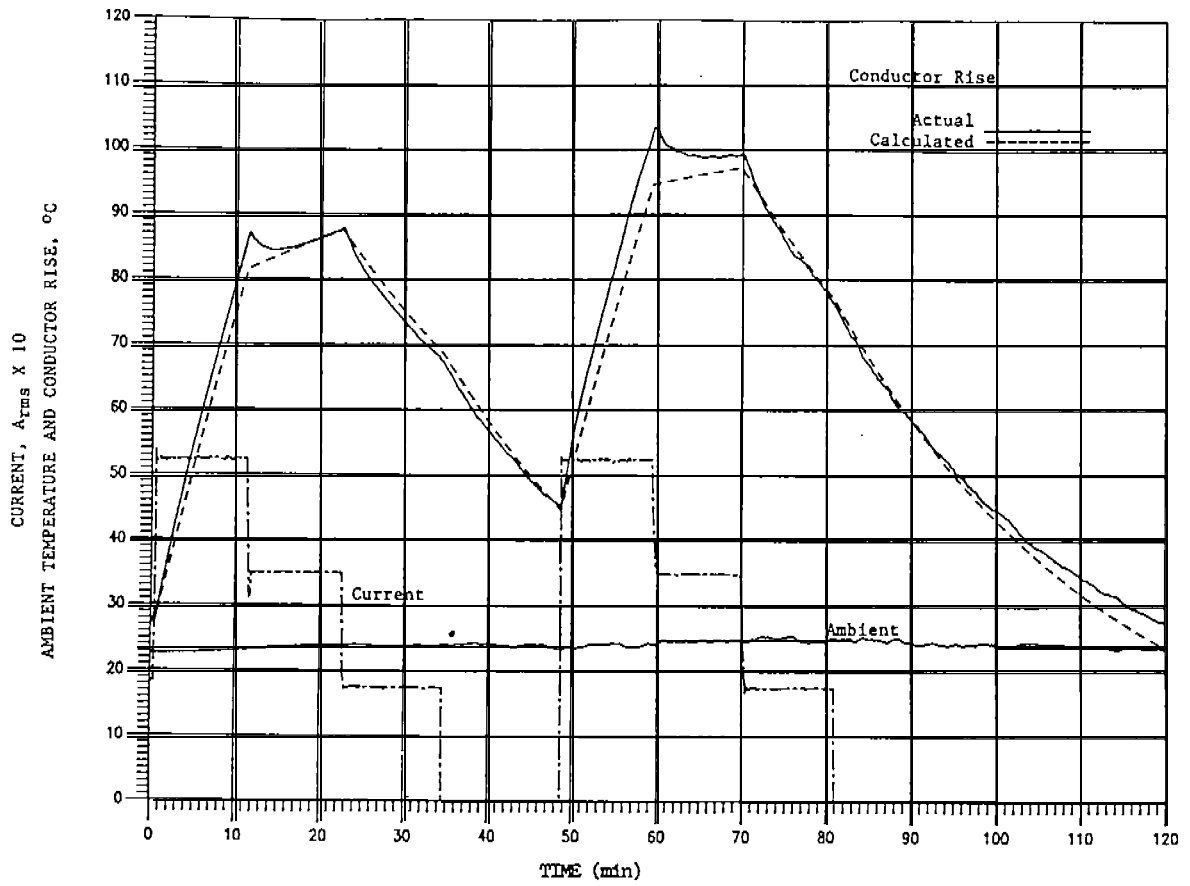


Fig. 2. Conductor temperature rise—four-step "high" current, 2/0 cable, round, type G-GC, 90°C.

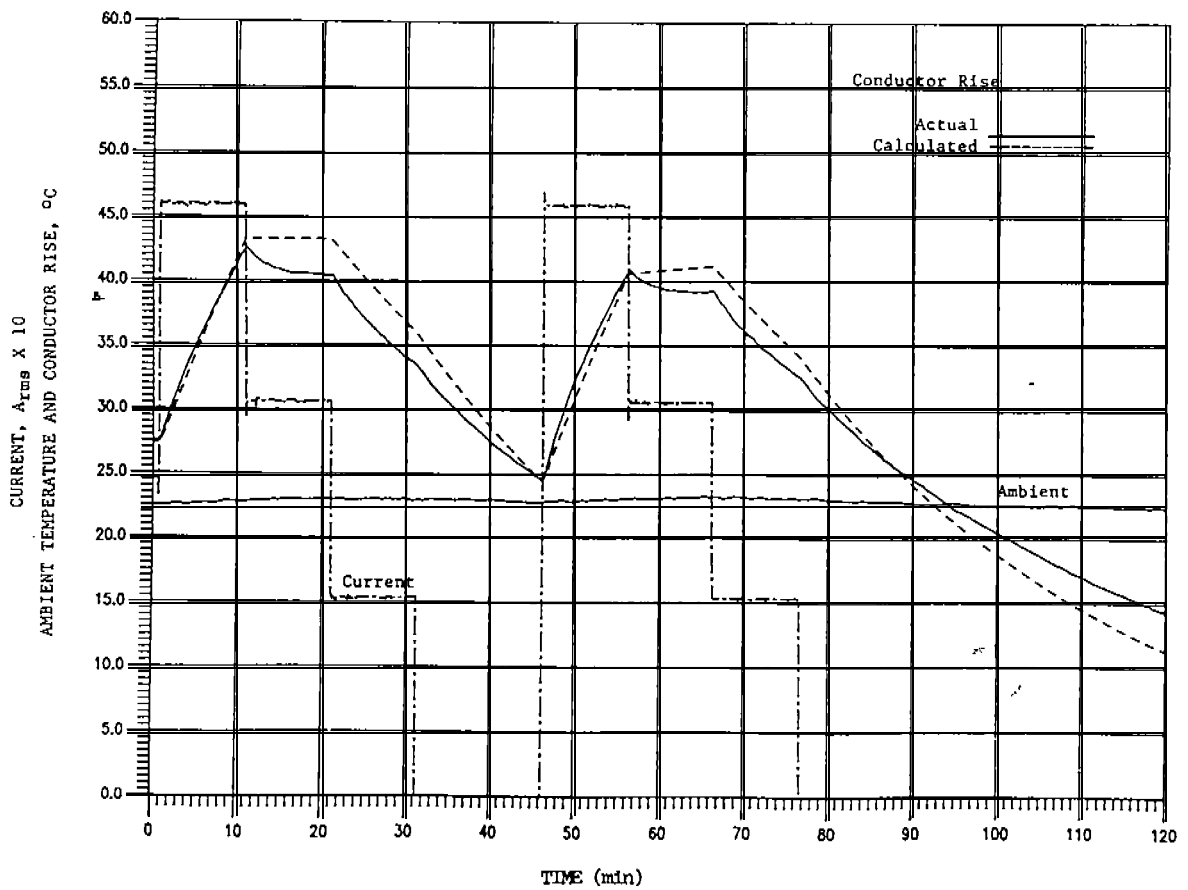


Fig. 3. Conductor temperature rise—four-step "low" current, 4/0 cable, round, type G-GC, 90°C.

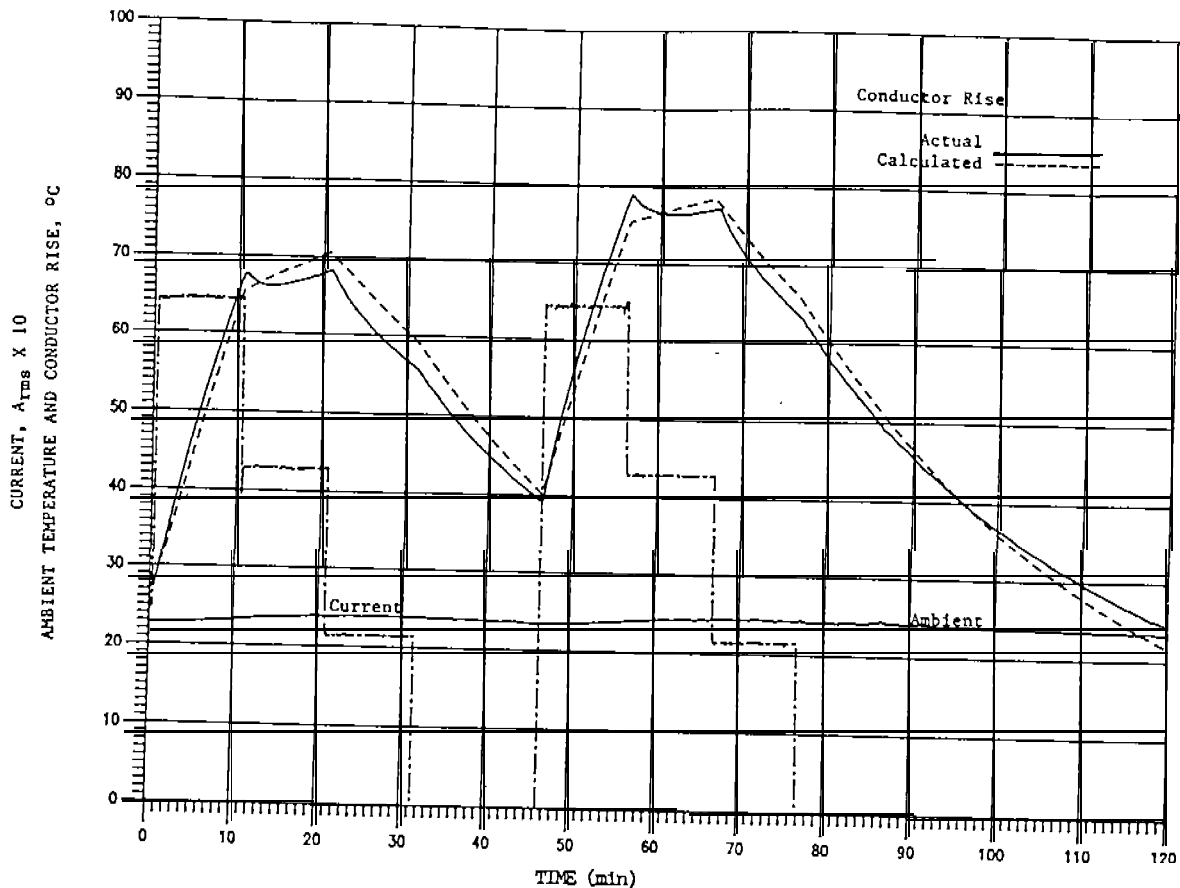


Fig. 4. Conductor temperature rise—four-step “high” current, 4/0 cable, round, type G-GC, 90°C.

were set to the actual value of $i(t)$ occurring at the end time of the 0.1-min section being calculated. Idealized ramp current equations were programmed on the computer, in effect smoothing the actual currents for the calculations. If the ramps are not converted to stepped constant currents and the 0.1-min calculation interval is retained, a plot of the T_c values so calculated are essentially indistinguishable from the calculated values in Figs. 5-8.

F. Discussion of Initial Test Results

The agreement between the actual and calculated conductor temperature rises in Figs. 1-4 is encouraging. An error common to all four figures is visible in the time intervals where current is zero—more so near the end time of each figure. In these regions the calculated conductor temperature rises depart from (become less than) the actual values at an increasing rate. This error is not due to the choice of K_d/K_c since the operative equation is (26)—which does not contain K_d/K_c . The values of T_{ai} and t_c are accordingly suspect. However, in these regions the figures show T_a is essentially constant. If t_c is the source of the error, it would appear that t_c increases as conductor temperature decreases. The ramp test results of Fig. 5-8 are also encouraging; the maximum error in predicting the conductor temperature is +4.6°C in Fig. 8. The cooling error discussed relative to Figs. 1-4 is also evident in Figs 5-8.

1) *Effect of Calculation Interval:* An analysis to determine the effect of the calculation interval was instructive. For

the constant current steps on Figs. 1-4, varying the calculation interval does not affect the calculated $T_c - T_a$ value. However, in Figs. 5-8, when (as was done) i_0 is set equal to i_T in (25), larger (more erroneous) T_c values are calculated as the calculation interval is increased. If the simplification $i_0 = i_T$ is not used, the T_c values so calculated agree well with the calculated T_c values in Figs. 5-8, independent of the calculation interval (0 to T); for example, at ramp end points, T_c values calculated from $i_0 = i_T$ for any T in the range 0.1 to 5 min agree within $\pm 1^\circ\text{C}$ overall with the calculated values in Fig. 5-8.

2) *Effect of “Running” I_{rms}* The effect of substituting “running (compound waveform) I_{rms} for I_{rms} in (38) was also analyzed. T_c values were calculated from (38) using running I_{rms} values and corresponding calculation intervals $t = (t \text{ to } T = (\text{successively}) 5, 10, 15, 20, 25, 30, \text{ and } 45 \text{ min})$. The “running I_{rms} ” T_c values agree with the calculated values in Figs. 5-8 to within -1°C and $+3.5^\circ\text{C}$ overall for time points 5, 10, 15, 20, 25, and 30. At 45 min, the “running I_{rms} ” T_c values range overall between 3.9°C and 7.2°C higher than the calculated values in Figs. 5-8.

III. CONCLUSION

Mathematical models were developed for real-time conductor temperature rise in 2/0 and 4/0 G-GC round trailing cables. A common equation represents both cables; only the parameters differ. The equation is not precise since current averaging and other approximating measures were employed in its

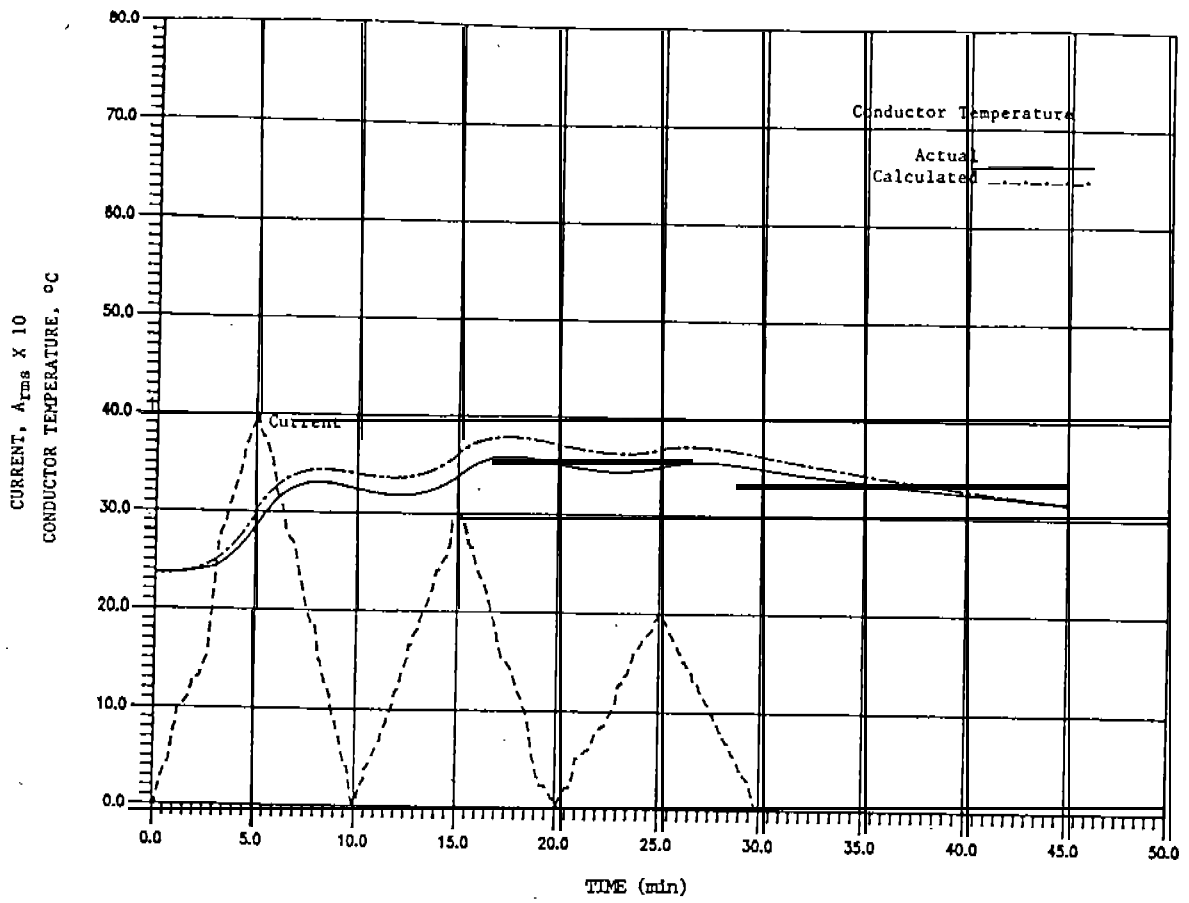


Fig. 5. Conductor temperature—ramp current, 2/0 cable, round, type G-GC, 90°C.

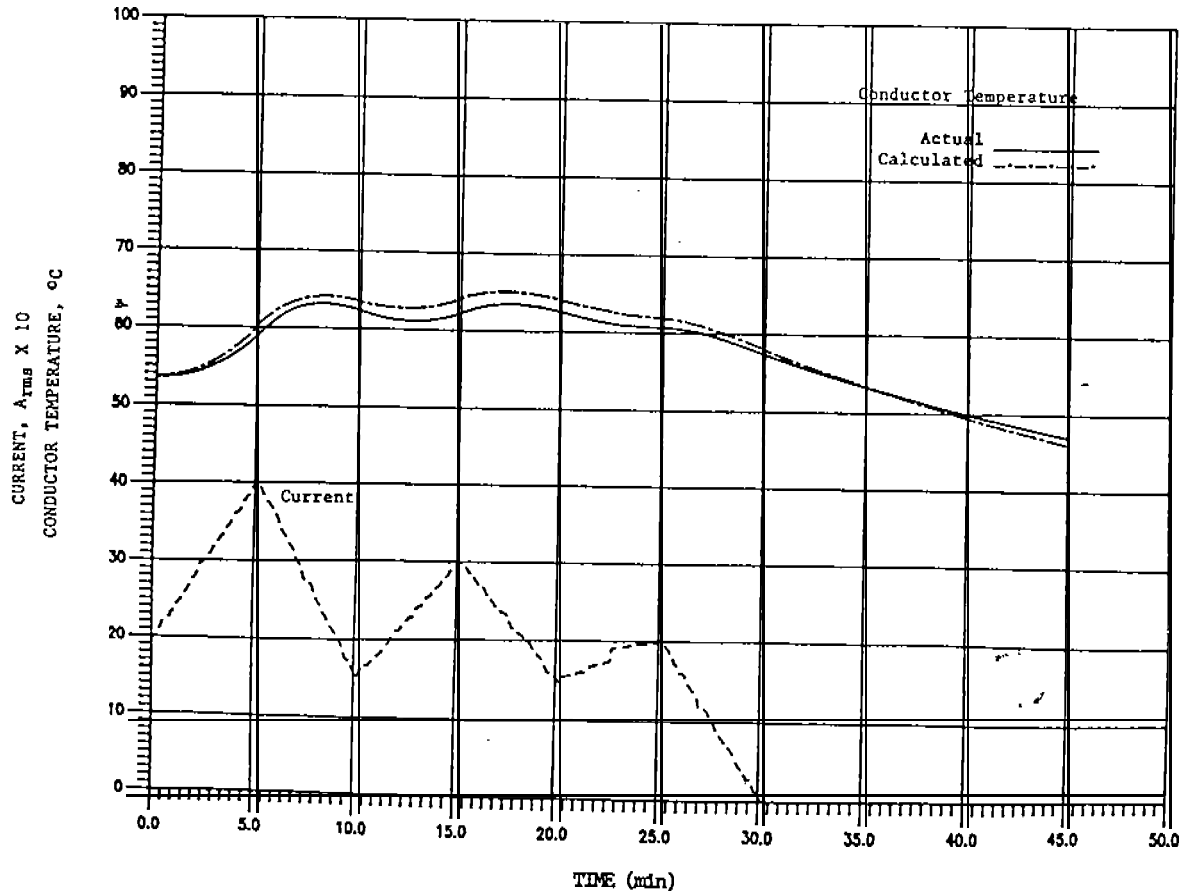


Fig. 6. Conductor temperature-ramp current, 2/0 cable, round, type G-GC, 90°C.

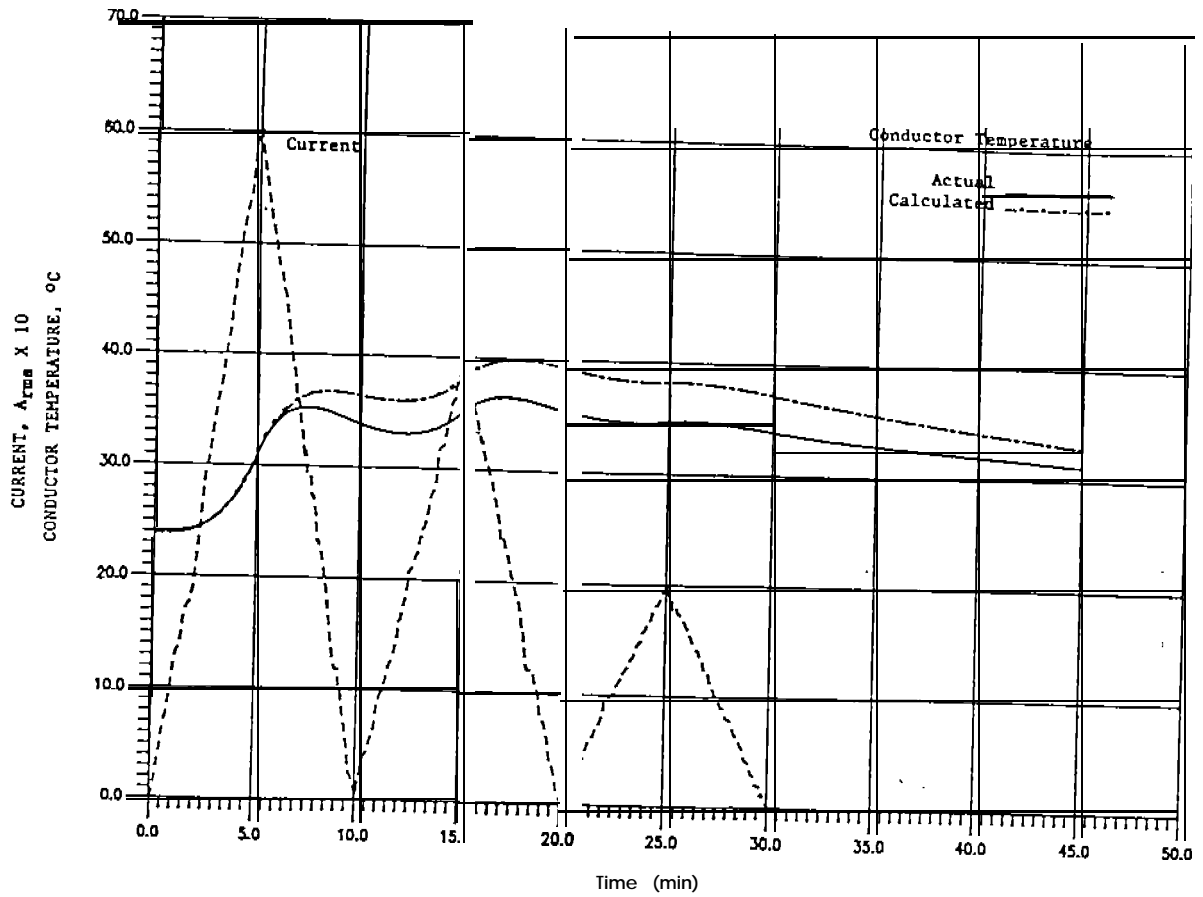


Fig. 7. Conductor temperature-ramp current, 4/0 cable, round, type G-GC, 90°C.

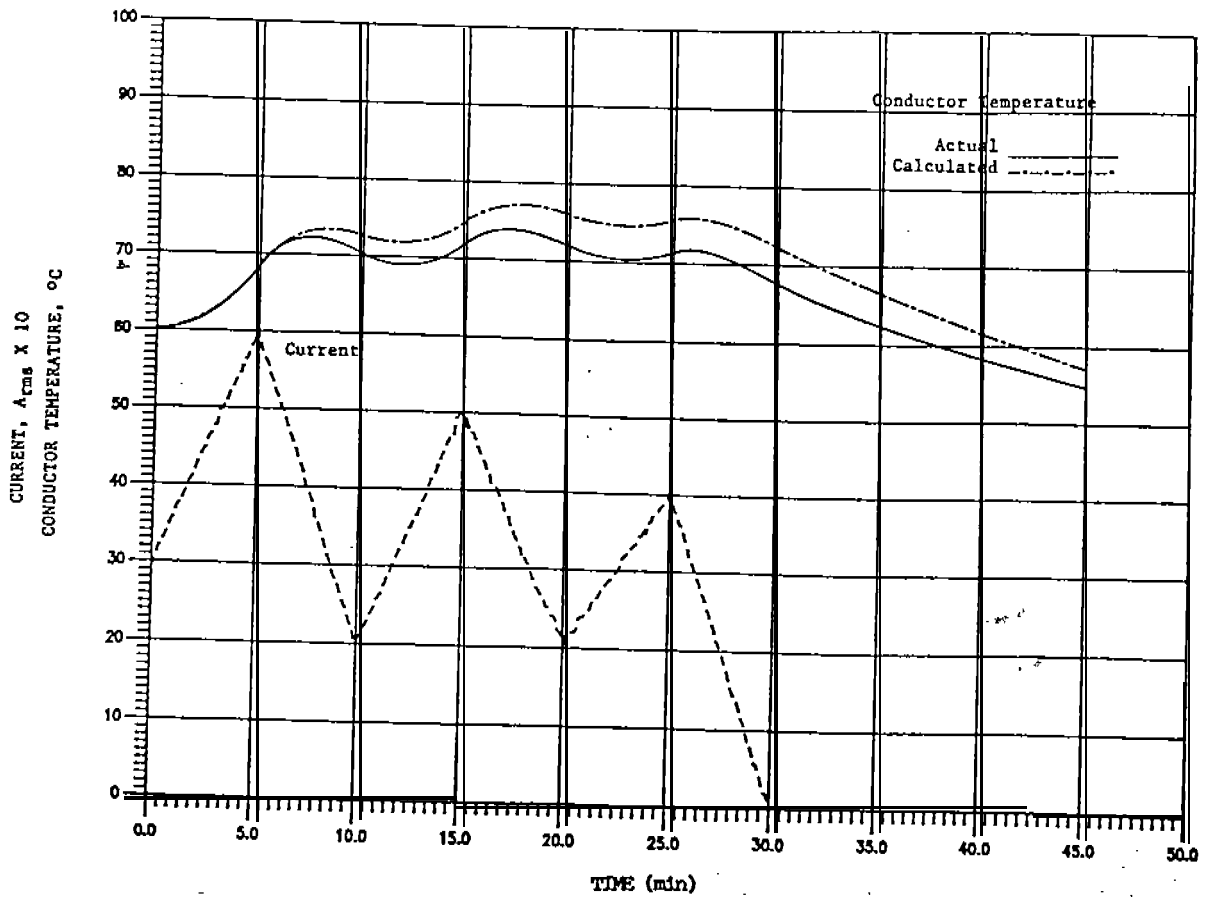


Fig. 8. Conductor temperature-ramp current, 4/0 cable, round, type G-GC, 90°C.

derivation. Methods were derived and implemented to measure the equation parameters, i.e., a presumed constant ratio (K_i/K_c) and a presumed cooling constant (t_c). For each cable, alternate measuring methods produced different K_i/K_c values, indicating that K_i/K_c may in fact not be constant. Of these values, a best-fit K_i/K_c was subsequently determined for each cable from dynamic trials using stepped constant current waveforms. Ramp current trials were also conducted thereafter. The results of both the stepped-constant current and ramp cut-rent trials are encouraging. A common error is evident in regions of pure cooling (i.e., where the current is zero), indicating that t_c may not be constant but variable with conductor temperature.

Model refinement effort is planned, primarily to resolve the evident inconstancy of K_i/K_c and t_c . Additionally, the cable models will be tested further in the laboratory on a series of current waveforms which simulates the fluctuating current conditions in the trailing cables. A means for signaling the demarcation of the various waveforms or waveform segments (based on slope change) will be incorporated beforehand. Contingent on success in these activities, trials will be conducted on an operating continuous miner.

ACKNOWLEDGMENT

The author wishes to express appreciation to Robert Conlin for general assistance, to Duane Wease who prepared the cable samples and monitored the cable tests, to Kenneth Myers who designed and assembled the automatic data collecting system and devised various computer programs for evaluating and graphing the test data, to Wayne Carey (who proofed the mathematics), to Judith Coulter (who critiqued the wording of the paper), and to Alicia Tyler for typing the many equations. Appreciation is also extended for helpful discussions with John W. Corm, Mark Fuller, Cablec Corporation (who provided the cables, gratis), and John Kovac (who critiqued the mathematical procedure), Peter Kovalchik, and Michael Yenchek, Pittsburgh Research Center, Bureau of Mines, Pittsburgh, Pennsylvania.

REFERENCES

- [1] M. R. Yenchek and P. G. Kovatchik, "Thermal characteristics of energized trailing cables," in *Proc. 9th WVU Int. Mining Electrotechnology Conf.*, July 26-29, 1988, pp. 178-185.
- [2] S. W. Melsom and H. C. Booth, "The rating of cables for intermittent or fluctuating loads," *J. Inst. Elec. Eng.*, vol. 61, pt. 1, pp. 363-368, Dec. 1922/Apr. 1923.
- [3] J. R. Cox, "Current ratings of trailing cables with particular reference to intermittent loads," *Mining Elec. Mech. Eng. (Proc. AMEME)*, VOL 32, pp. 143-151, Nov. 1951.
- [4] *Mining Cable, Engineering Handbook*, Cablec Corporation 1988.
- [5] L. M. Kells, *Elementary Differential Equations*. New York: McGraw-Hill, 1954.
- [6] G. W. Luxbacher, "Evaluation of the effectiveness of molded-case circuit breakers for trailing cable protection," Ph.D. dissertation in Mining Engineering, The Pennsylvania State University, Nov. 1980.
- [7] *Thermocouple Reference Tables*, NBS Monograph 125, Nat. Bur. of Standards, Washington, DC, 1979.
- [8] *Practical Temperature Measurements*, HP Application Note 290, Hewlett-Packard Company, III Zeta Drive, Pittsburgh, PA, Aug. 1980.



John M. Mesina received the B.S.E.E. degree (Cum Laude) from the University of Pittsburgh, Pittsburgh, PA.

He served in the U.S. Navy as an Aviation Electronics Technician, and while in school he held the position of Technician for the University of Pittsburgh's Engineering Research Division and for the Mellon Institute. He then worked for 23 years as a Research and Senior Research Engineer, specializing in the design and development of automated nondestructive-test instrumentation systems for production line application at the Jones and Laughlin Steel Company (later absorbed by the LTV Corporation). He joined the Mine Safety and Health Administration (MSHA), Directorate of Technical Support at the Approval and Certification Center, Triadelphia, WV, in 1983. His activities at MSHA include investigation work in the areas of microprocessor devices, high-voltage criteria, cable ampacity, short circuit and arcing fault calculations, and splice characterization. He has published papers in Materials Evaluation, Instrumentation in the Iron and Steel Industry (ISA), and in the *Proceedings of the Ninth WVU International Mining Electrotechnology Conference*. He shares US Patent 3,986,389.

1000
1000